Available online at www.sciencedirect.com
SCIENCE DIRECT®
Journal of Photochemistry and Photobiology A: Chemistry 158 (2003) 69–76
Journal of Photochemistry and Photobiology A:Chemistry
www.elsevier.com/locate/jphotochem

Control of photodissociation: vibrational mode selection and quantum interference

Hideki Ohmura, Taisuke Nakanaga*

Photoreaction Control Research Center, National Institute of Advanced Industrial Science and Technology (AIST), Higashi 1-1, Tsukuba, Ibaraki 305-8565, Japan

Received 26 April 2002; received in revised form 25 October 2002; accepted 25 October 2002

Abstract

We present two methods for using lasers to control the photodissociation of small molecules and molecular complexes. The first method, which involves ternary aniline cluster cations consisting of aniline, water, and an aromatic molecule (benzene or pyrrole), utilizes the strong interaction between an NH stretching vibration and an adjacent hydrogen bond The infrared predissociation reactions of the cluster cations were investigated. Upon absorption of an infrared photon, the clusters dissociated and eliminated either water or the aromatic molecule. Measurements of the branching ratio for this reaction revealed that fission of the hydrogen bond was accelerated by excitation of the NH stretching vibration adjacent to the targeted hydrogen bond. The second method involves coherent control in the frequency domain. We investigated interference effects on the two-color dissociation of IBr using the fundamental (560 nm) and its second harmonic (280 nm). In the strong-excitation regime by the fundamental light ($\sim 1.3 \times 10^{10}$ W cm^{-2}), the yield of iodine atoms from IBr oscillated with the relative phase of the 560 and 280 nm light, whereas no change was observed in its angular distribution. This phase-dependent behavior can be explained by interference between the one-photon transition induced by the second-harmonic light and the dipole-forbidden two-photon transition induced by the strong fundamental light.

Keywords: Hydrogen bond; Mode selective photo-dissociation; Coherent control; Photo-dissociation

1. Introduction

Laser chemists have long dreamed of using monochromatic lasers to break targeted bonds with the precision of a scalpel. In spite of their efforts, there has been only one report of this kind of control; Butler et al. [1,2] studied the dissociation of CH_2IBr—which has two possible paths: $CH_2IBr \rightarrow CH_2I + Br$ and $CH_2IBr \rightarrow CH_2Br + I$—and found that the stronger bond, C–Br, dissociated selectively when the molecule was irradiated with a UV laser (210 nm). But this kind of selectivity has been reported only for this molecule, and the weaker bond, C–I, always dissociates in larger or more complex haloalkanes, probably owing to fast energy relaxation or to differences in the strengths of the intramolecular interactions in the excited electronic states. To circumvent these problems, we propose two approaches for controlling laser-induced photoreactions: (1) mode-selective infrared predissociation of hydrogen-bonded clusters and (2) coherent control of the photodissociation of simple molecules in the frequency domain [3].

Our first approach began with a simple question. Is it really impossible to control photoreactions by old-fashioned selection of the absorption frequency? To answer this question, we adopted as a model reaction the infrared photodissociation of the hydrogen bond in some ternary aniline clusters. In these clusters, the hydrogen bond is the intermolecular interaction between an XH (X = O, N) bond and either a nonbonding orbital (σ-type) or a π-electron (π-type); such interactions play important roles in various chemical and biological substances [4].

Fig. 1 shows the infrared spectra of isolated aniline clusters in supersonic jets. The figure clearly indicates that the NH stretching bands broaden and undergo a large red shift when hydrogen bonds are formed. There are several reasons for this well-known behavior [4]. This broadening occurs in the isolated clusters, which suggests that it is a homogeneous broadening; that is, it is due to fast energy transfer from the NH stretching vibration to the adjacent hydrogen bond. The large bandwidth (50–100 cm^{-1}) indicates that the lifetime of the excited state is less than 1 ps if the interaction is strong. This relaxation lifetime is much shorter than that of the usual intramolecular vibrational energy redistribution (IVR) lifetime (∼10 ps), and therefore we can hope

* Corresponding author. Tel./fax: +81-298-54-4521.
E-mail address: t.nakanaga@aist.go.jp (T. Nakanaga).

1010-6030/03/$ – see front matter © 2003 Elsevier Science B.V. All rights reserved.
doi:10.1016/S1010-6030(03)00019-4

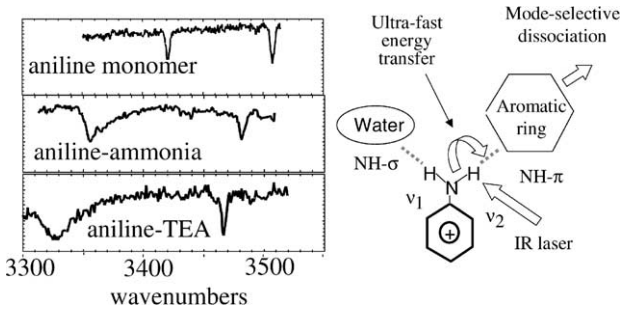

Fig. 1. Infrared spectra of isolated aniline clusters in the NH_2 stretching vibration region and ultra-fast energy relaxation between the NH stretching vibration and the intermolecular vibration.

to control the fission of the hydrogen bond by exciting the XH stretching vibration adjacent to the hydrogen bond. We have already reported that the branching ratio depends on the excited vibrational modes of the aniline–water–benzene and aniline–water–pyrrole cations [4,5]. In this paper we will discuss the role of fast energy transfer from the NH vibration to the adjacent hydrogen bond.

The second approach to laser-selective chemistry is the coherent control technique. This approach has been widely investigated because it has the potential to prevent rapid internal energy redistribution, which has invalidated traditional mode-selective chemistry [7,8]. The coherent control technique can be roughly classified into two approaches, a time-domain approach and a frequency-domain approach. For the purposes of this research, we adopted the latter approach.

The frequency-domain approach is based on manipulation of the interference between two or more optical transitions. This approach can be understood in terms of an analogy to Young's double-slit experiment, in which constructive or destructive interference promotes or suppresses the target reaction path, respectively. Shapiro et al. [3] have reported a strategy that uses the interference between a dipole-allowed three-photon transition induced by the fundamental light and a one-photon transition induced by the third-harmonic light. This type of interference has been observed experimentally in the ionization of atoms [9] and diatomic [10,11] and polyatomic molecules [12–14]. Zhu et al. [15–17] have demonstrated control of the branching ratio between photoionization and photodissociation of HI molecules. However, experiments on selective photodissociation are still limited by their dependence on the availability of suitable laser frequencies and systems that have intermediate energy levels that are appropriate for the observation of a weak three-photon transition. The interference between a one-photon transition induced by the second-harmonic light and a two-photon transition induced by the fundamental light has also been investigated and applied to various systems [18]. Because in this case the final states have different selection rules, owing to the different parity of the two transitions, we can control only the angular distribution of the dissociated products, not the dissociation yield [18]. However, recent theoretical work has proposed the use of a static electric field to achieve nearly complete phase control of the total ionization (or dissociation) yield, control that results from interference between the dipole-forbidden two-photon transition and the corresponding one-photon transition induced by second-harmonic light [19]. This work has shown that applying the external field to prepare mixed states with opposite parity in the intermediate state may make general phase control possible.

We have already observed the interference effect in the generation of iodine atoms in the excited state by two-color dissociation of IBr using the fundamental (560 nm) and its second-harmonic (280 nm) radiation [20]. In this paper, we will discuss the mechanism of the interference effect in IBr and will apply the same method to the generation of ground-state iodine atoms to determine whether control of the photodissociation of IBr is possible.

2. Mode-selective infrared predissociation of the hydrogen-bonded clusters

2.1. Experimental

Fig. 2 shows the principle of the infrared depletion method, which we used to measure the infrared predissociation of the hydrogen-bonded cluster cations. The details of the experimental setup have been described elsewhere [5,21]. The ternary aniline clusters were generated in the cluster beam by injection of a premixed gas containing He, aniline, water, and pyrrole or benzene into the high-vacuum chamber through a pulsed valve (Ø0.8 mm, duration ≈250 μs). The cluster beam was introduced into the ionization chamber of the time-of-flight (TOF) mass spectrometer through a molecular beam skimmer (Ø1 mm). The neutral cluster was ionized by near-resonant two-photon absorption of UV laser light (REMPI method), and the cluster cation was detected with a homemade linear TOF mass spectrometer ($L = 0.5$ m).

The cluster cation was dissociated with an infrared laser beam generated by difference-frequency mixing of the fundamental output of a Nd:YAG laser (Spectra Physics GCR-III) and the output of a dye laser (Spectra Physics PDL-3, Dye: LDS765). This infrared laser emits infrared light that

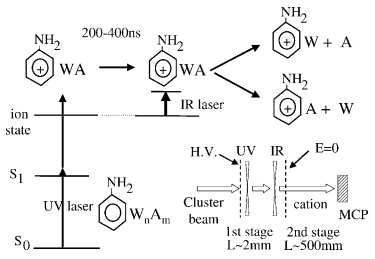

Fig. 2. Principle of the infrared depletion method used for the measurements of the branching ratios.

is stronger than 0.5 mJ/pulse in the 3200–4000 cm^{-1} region. The decrease of the original cluster cation and the generation of fragment cations in the mass spectrum were measured, and the branching ratio was determined. In the measurement, the infrared light was focused at about 2 mm downstream in the cluster beam from that of the UV laser in the acceleration region of the TOF spectrometer, and the delay time between the two lasers was set to ∼300 ns so that the flight time of the fragment cation produced by infrared predissociation would differ from that of the original cation of the same mass [5]. This method enabled us to measure the intensity of the mass signal of the product cation correctly.

The branching ratio, R = (aniline–water$^+$/aniline–aromatic$^+$), was determined as the ratio of the cationic products of the following reactions:

$$\text{aniline–water–aromatic}^+ \rightarrow \text{aniline–water}^+ + \text{aromatic}$$

$$\text{aniline–water–aromatic}^+ \rightarrow \text{aniline–aromatic}^+ + \text{water}$$

when the infrared laser light was too strong, the effect of sequential two-photon absorption was observed; the fragment cation absorbed the second infrared photon and dissociated into aniline$^+$ and water or aniline$^+$ and aromatic. To avoid this effect of the multi-photon dissociation, we plotted the signal intensity of the fragment cation against the infrared laser power and used only the first-order portions to estimate the reaction rate. By using the standard deviations obtained from more than 10 measurements of the power dependence of the mass signal, we estimated the experimental error in the branching ratio for both clusters to be about 0.02. The error came mainly from fluctuation in the conditions of the cluster beam.

2.2. Results and discussion

Our reasons for adopting the ternary cluster cations of aniline, water, and an aromatic molecule (benzene or pyrrole) as models for studying the mode-selective infrared photodissociation were as follows:

(1) The structures and intermolecular interactions of aniline clusters are well understood.
(2) Measuring the branching ratio of the photodissociation of cluster cations is easier than measuring the ratio of neutral clusters.
(3) The strength of the interaction of the NH-σ type hydrogen bond between NH and water and that of the NH-π type hydrogen bond between NH and an aromatic ring are almost the same, and two reaction paths are observed in the infrared predissociation reaction of the ternary cluster cations.
(4) The red shift in the NH stretching vibration caused by the NH-σ hydrogen bond differs from the shift caused by the NH-π hydrogen bond, and therefore we can excite the NH bond adjacent to the target hydrogen bond without exciting the other one.

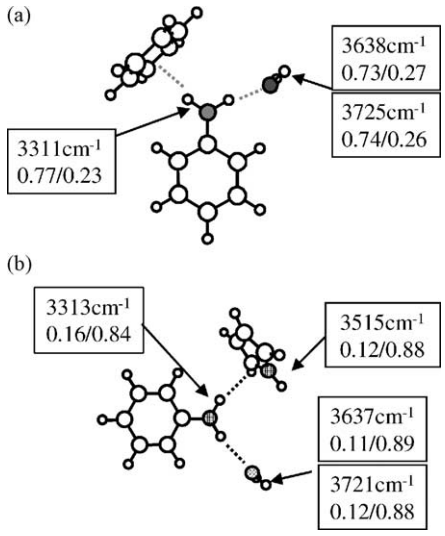

Fig. 3. Branching ratio of the infrared predissociation of the aniline–water–pyrrole cluster cation. (a) Aniline–water–benzene cation, $R = AW^+/AB^+$; (b) aniline–water–pyrrole cation, $R = AW^+/AP^+$. A: aniline, W: water, B: benzene, P: pyrrole.

We have measured the infrared spectra and the branching ratios of the infrared predissociation reactions of aniline–water–benzene and aniline–water–pyrrole cations, and the results are summarized in Fig. 3. The structures of the cluster cations and assignments of the infrared bands shown in the figure were confirmed by means of molecular orbital calculations using the DFT method (Gaussian 98, B3LYP/6-31++G**) [22]. It has been found that the branching ratio measured for the NH stretching vibration interacting with an aromatic molecule is different from the ratios measured for the other vibrational modes [5,6].

Fig. 3a shows the branching ratio for the infrared predissociation reaction of the aniline–water–benzene cation measured for the vibrational modes in the 3800–3200 cm^{-1} range [5]. This cluster has three infrared bands, at 3311, 3638, and 3725 cm^{-1}, in this region. They were assigned to the stretching vibration of NH interacting with benzene and the symmetric and antisymmetric stretching vibrations of the OH bond of water whose oxygen atom was interacting with NH, respectively. As seen in Fig. 3a, the main product of the reaction was the aniline–water cation, although the proton affinity of water (697 kJ/mol) is smaller than that of benzene (759 kJ/mol) [23]. This difference is due to the nature of the NH-σ type and NH-π type hydrogen-bonding interactions.

It is interesting that the branching ratio observed for the stretching vibration of NH interacting with benzene (0.77/0.23) is larger than the ratios observed for the OH stretching vibrations (0.73/0.27, 0.74/0.26). The difference is larger than the experimental error (0.02). There are two possible explanations for this difference. One is fast energy transfer from the NH stretching vibration to the intermolecular hydrogen bond adjacent to the NH bond. The vibrational energy of the NH stretching mode moves to the

hydrogen bond and causes it to break. The other explanation is the difference of the excess energies of the two reactions. The yield of the main product (aniline–water cation) may increase when the lower-frequency band is excited and the excess energy becomes smaller.

Fig. 3b shows the results of the measurement for the aniline–water–pyrrole cation. This cluster has four infrared bands, at 3313, 3515, 3637, and 3721 cm^{-1}, in the 3800–3200 cm^{-1} region. These bands were assigned to the stretching vibration of the NH of aniline interacting with pyrrole, the NH stretching vibration of pyrrole, and the symmetric and antisymmetric stretching vibrations of water whose oxygen atom was interacting with NH, respectively. The main product of the reaction was the aniline–pyrrole cation in this case. The difference between this reaction and the reaction of the aniline–water–benzene cation can be explained by the difference in the proton affinities of pyrrole (868 kJ/mol) and benzene (759 kJ/mol) [23].

The branching ratio of the reaction observed for the NH stretching vibration (0.16/0.84) is definitely larger than the ratios obtained for the OH stretching vibrations (0.11/0.89, 0.12/0.88) and the NH stretching vibration of pyrrole (0.12/0.88). The difference between the NH stretching vibration and the other vibrations is larger than the experimental error (0.02), as was true for the aniline–water–benzene cation. However, in this case the aniline–water cation was the by-product and should be unstable relative to the aniline–pyrrole cation. Fig. 4 is a schematic diagram of the relative energy of the fragment ions and the excitation energies. Since the frequency of the NH stretching vibration is the lowest of the four vibrational modes, the ratio of the unstable product to the stable product increases at the minimum excitation energy. This result confirms the idea that ultra-fast energy transfer from the NH stretching vibration to the intermolecular vibration accelerates the infrared predissociation of the hydrogen bond.

It is interesting that the branching ratio obtained for the NH stretching vibration of pyrrole agreed with that obtained for the OH stretching vibrations of water. In the former case, the pyrrole molecule was excited, and the excess energy should pass through the NH bond of aniline interacting with pyrrole. In the latter case, the water molecule is excited, and the excess energy also should pass through the other hydrogen bond, between water and NH bond. The fact that branching ratios for the NH of pyrrole and the OH of water are the same suggests that the IVR is really fast, and the usual conclusion that no mode selectivity can be expected stands for the ordinary vibrational modes such as the free NH and free OH stretching vibrations. In other words, the energy transfer from the NH stretching vibration to the adjacent hydrogen bond is much faster than the other relaxation mechanism.

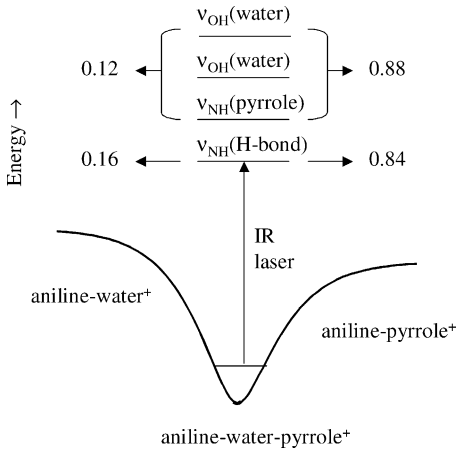

Fig. 4. Schematic diagram of the relative stabilities of the fragment ions and the excitation energy.

3. Coherent control of the photodissociation of IBr

3.1. Experimental

The configuration of the experimental apparatus used for the coherent control of the photodissociation of IBr is given in detail elsewhere [20]. The dye laser, which was pumped by the frequency-doubled output of a Q-switched Nd:YAG laser, produced a 100 mJ, 10 ns pulse at 560 nm with a linewidth of 0.1 cm^{-1} (Lambda Physik, SCANMATE). We inserted a phase-matched frequency-doubling crystal (β-barium borate, type-I phase-matching), producing an ultra-violet beam at $\lambda = 280$ nm. After the second-harmonic generation (SHG), the beam was separated into the second-harmonic light and the fundamental light by means of a UV dielectric mirror in the Mach–Zehnder interferometer. We inserted absorption filters in the path of the fundamental light to optimize the fundamental power. We also placed a half-wave plate that rotated the polarization of the fundamental light by approximately 90°, so that the polarizations of the two fields were parallel to each other. The fundamental beam passed through an antireflection-coated quartz plate (thickness: 0.25 mm) that could be rotated. This plate was used to change the relative phase of the two fields, and the double-pass configuration was employed to avoid lateral beam shift. After being recombined, the two beams were introduced into the reaction chamber.

The reaction chamber consisted of a supersonic beam source and a homemade TOF spectrometer. The molecular beam went through a skimmer (diameter: 1.0 mm) located 20 mm from the nozzle. With a 10 Hz repetition rate and a stagnation pressure of 50 kPa, the pressure in the chamber was kept below 3.0×10^{-4} Pa. After passing through the skimmer, the molecular beam was intersected at right angles by the fundamental and the second harmonic, whose polarizations were parallel to the detection axis. The second-harmonic light played two roles: photodissociation of IBr in the UV region and ionization of the spin–orbit excited iodine atoms that dissociated from IBr. The iodine fragments were ionized by 2 + 1 REMPI using the following electronic transition: $I^*(5p; {}^2P^0_{1/2}) + 2h\nu$ (λ =

280.69 nm) → I(8p; $^2D^0_{5/2}$) [24]. The ions were detected by means of a microchannel plate. The signal was averaged over 512 runs. We performed one-dimensional photofragment translational spectroscopy on the spin–orbit excited iodine atoms.

The IBr sample was obtained from Aldrich and used without further purification. The gas sample for the molecular beam was prepared by passing He gas over solid IBr (which has a vapor pressure of ∼400 Pa at room temperature) for a total pressure of ∼0.1 MPa. We minimized the contributions from higher clusters by choosing only the initial part of the molecular beam pulse.

3.2. Results and discussion

The absorption spectrum of IBr at room temperature has two main bands, centered at 270 and 500 nm [25], as shown in Fig. 5a. IBr has four available dissociation pathways, which are shown below in order of increasing energy of the separate atoms:

$$IBr + h\nu \rightarrow I(^2P_{3/2}) + Br(^2P_{3/2})$$

$$IBr + h\nu \rightarrow I(^2P_{3/2}) + Br^*(^2P_{1/2})$$

$$IBr + h\nu \rightarrow I^*(^2P_{1/2}) + Br(^2P_{3/2})$$

$$IBr + h\nu \rightarrow I^*(^2P_{1/2}) + Br^*(^2P_{1/2})$$

where $I(^2P_{3/2})$ and $Br(^2P_{3/2})$ are the ground states and $I^*(^2P_{1/2})$ and $Br^*(^2P_{1/2})$ are the spin–orbit excited states. For convenience, these states will be denoted simply as I, Br, I*, and Br*, respectively, and the dissociation channels will be denoted simply as I + Br, I + Br*, I* + Br, and I* + Br*. The photodissociation dynamics of IBr can be roughly divided into two regimes: the visible region and the UV region. In the visible region, the I + Br and I + Br* channels are available. The diagram of relevant potential energy curves and corresponding dissociation channels is shown in Fig. 5b. The ground state of IBr has the configuration $(\sigma)^2(\pi)^4(\pi^*)^4(\sigma^*)^0$ and the term symbol $^1\Sigma_{0+}(2440)$, where the (*ijkl*) suffix in the term symbol is an abbreviated notation for the configurations $(\sigma)^i(\pi)^j(\pi^*)^k(\sigma^*)^l$. The main oscillator strength is assigned to the transition to the bound $^3\Pi_{0+}(2431)$ state (B state), which dissociates to produce I + Br*. I + Br is produced via an avoided crossing of the bound $^3\Pi_{0+}(2431)$ state with the repulsive $^3\Sigma_{0+}(2422)$ state, which correlates with the I + Br channel [26,27].

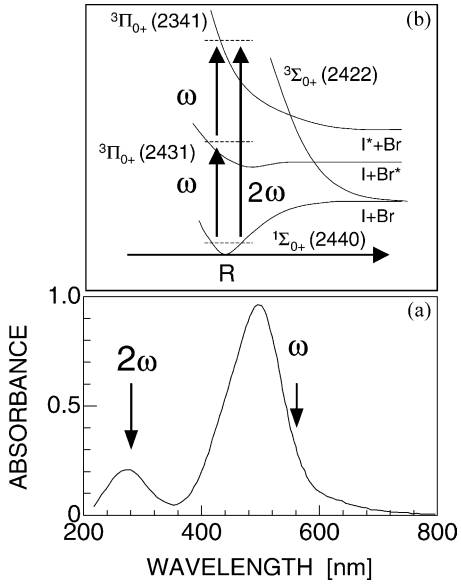

Fig. 5. (a) Absorption spectrum of IBr. The arrow shows the excitation wavelength of the fundamental light and the second-harmonic light. (b) Diagram of relevant potential energy curves and corresponding dissociation channels. For clarity, only the relevant states are shown.

In the UV region, the I + Br, I + Br*, and I* + Br channels are available. Recent experimental studies have assigned the UV band to the overlapping of the $^3\Pi_1(2341)$, $^3\Pi_{0+}(2341)$ and $^1\Pi_1(2341)$ states. Only the $^3\Pi_{0+}(2341)$ state correlates to the I* + Br channel [28–30]. We tuned the wavelengths of the fundamental and the second-harmonic light as shown by the arrows in Fig. 5a.

Fig. 6a shows the TOF spectrum of I* produced from photodissociation of IBr at 280 nm. Two peaks are observed in the TOF spectrum, which reflects an anisotropic dissociation. The first peak of the signal corresponds to I* atoms whose initial recoil velocities are toward the MCP detector, and the second peak corresponds to I* atoms whose velocities are away from the MCP detector. To obtain information about the symmetry of the excited state, we analyzed the line shape of the TOF spectrum. The velocity distribution of the photofragment along the detector axis, *Z*, is given by the following equation [31]:

$$I(v_z, \alpha) = \int_v^\infty \frac{1}{4\pi} f(v)(1 + \beta P_2(\cos\alpha)), \quad (1)$$

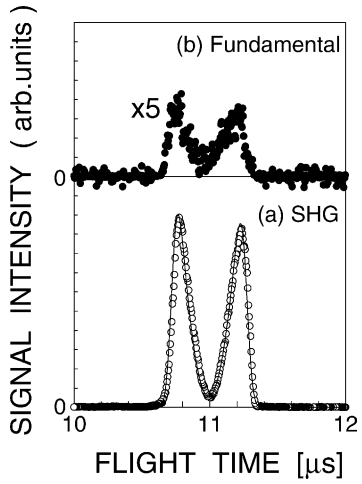

Fig. 6. (a) TOF spectrum of spin–orbit excited iodine atoms dissociated from IBr molecules at 280 nm. The solid line shows the least-squares fit of the TOF spectrum obtained by using Eq. (1). (b) TOF spectrum of spin–orbit excited iodine atoms dissociated from IBr molecules at 560 nm under the strong excitation for fundamental light (1.3×10^{10} W cm^{-2}).

where $P_2(x) = (3x^2 - 1)/2$ is the second-order Legendre polynomial, β is the anisotropy parameter of dissociation, α is the angle between the electric vector of the linearly polarized photodissociation laser and the photofragment recoil direction, and $f(v)$ is the initial velocity distribution of the photodissociation. The electronic configurations of IBr are described by term symbols Ω according to spin–orbit couplings, where Ω is the projection value of the total electronic angular momentum along the internuclear axis. The parallel transition corresponds to $\Delta\Omega = 0$ and the perpendicular transition to $\Delta\Omega = \pm 1$, where $\Delta\Omega$ is the difference between the values in the excited and the ground electronic states. If the dissociation is prompt, the two transitions give the two limiting values for β, i.e., $\beta = 2$ for the parallel transition and $\beta = -1$ for the perpendicular transition. The solid curve in Fig. 6a shows the result of the least-squares fit to Eq. (1) when β was taken as an adjustable parameter. Using $\beta(\mathrm{I}^* + \mathrm{Br}) = 1.89 \pm 0.05$, which is very close to the value of a parallel transition, the TOF spectrum can be well fitted to Eq. (1). This result is in good agreement with the results of an earlier experimental study that found that the parallel transition to the $^3\Pi_{0+}(2341)$ state yields $\mathrm{I}^* + \mathrm{Br}$ [30].

Fig. 6b shows the two-photon absorption signal that appeared in addition to the one-photon absorption signal when both the fundamental and the second-harmonic beams were irradiated. We could not detect this additional signal in the weak excitation by the fundamental light (less than $5 \times 10^9\,\mathrm{W\,cm^{-2}}$). Since the $\mathrm{I}^* + \mathrm{Br}$ channel does not open at 560 nm, only the $\mathrm{I} + \mathrm{Br}$ channel is open via the transition to the $^3\Pi_{0+}(2341)$ and $^3\Pi_1(2341)$ states [27]. By increasing the excitation intensity of the fundamental light to more than $5 \times 10^9\,\mathrm{W\,cm^{-2}}$, we were able to detect the small amount of additional I^* signal (8% of the SHG signal). We obtained the signal in Fig. 6b in the strong excitation for fundamental light ($1.3 \times 10^{10}\,\mathrm{W\,cm^{-2}}$) by subtracting the SHG signal from the total signal. A strong excitation higher than $1.3 \times 10^{10}\,\mathrm{W\,cm^{-2}}$ causes the ionization of IBr molecules by the fundamental light alone, then producing the $(\mathrm{I}^*)^+$ atom dissociated from IBr^+; and the observable range was very narrow (5×10^9 to $1.3 \times 10^{10}\,\mathrm{W\,cm^{-2}}$) and very close to the threshold for IBr ionization. The $^3\Pi_{0+}(2341)$ state correlated with the $\mathrm{I}^* + \mathrm{Br}$ channel can be reached by a multiphoton excitation by the fundamental light, and the $\mathrm{I}^* + \mathrm{Br}$ channel opens. Comparison of Fig. 6a and b shows that the spacing of the two peaks in the fundamental excitation is equal to that in the SHG excitation, which indicates that the momentum distribution of I^* atoms formed by the irradiation by the fundamental light is the same as that formed by the second-harmonic light. If a process involving more than two photons occurs, the component of larger momentum distribution should be observed in the iodine products. This result suggests that the final state of the transition induced by the fundamental light is the same as that of the one-photon dissociation induced by the second-harmonic light. There remains a possibility that although the energy levels of the two transitions are the same, their parities may be different. We will discuss this point later.

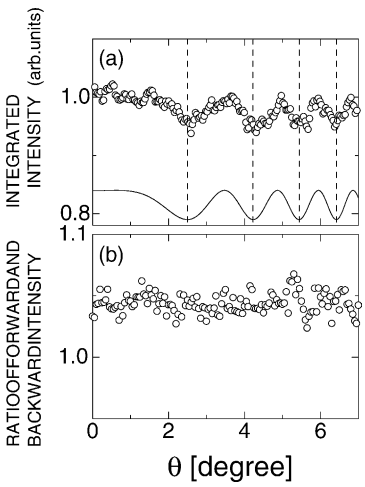

Fig. 7. (a) Dissociation yield of spin–orbit excited iodine atoms as a function of the quartz plate rotation angle, θ. The quartz plate was rotated to vary the relative phase between the fundamental light and the second-harmonic light. The solid curve shows the function $A + B\cos(\Delta\Phi + \Phi_0)$, where A, B, and a_0 are the adjustable parameters. The broken lines are the guides for eyes to show the period of the oscillation. (b) Ratio of the forward and backward yields, $R = I_\mathrm{f}/I_\mathrm{b}$, as a function of the quartz plate rotation angle, θ.

Fig. 7a shows the integrated signal of I^* atoms obtained when we changed the relative phase between the fundamental and the second-harmonic lights by rotating the quartz plate. The oscillating behavior is clearly observed. The contrast of oscillation C, defined as $C = (I_\mathrm{max} - I_\mathrm{min})/(I_\mathrm{max} + I_\mathrm{min})$, is 0.02 ± 0.005. We examined the oscillation of the signal carefully to confirm that it was caused not by some artifact such as fluctuation of the laser intensity but by interference between the two excitations.

The total electric field, E, of the coherent light waves exciting the molecule is

$$E(t) = E_1\cos(\omega t + \varphi_1) + E_2\cos(2\omega t + \varphi_2). \tag{2}$$

If we regard this field as a perturbation and take into account terms up to the second order, the excitation probability can be written as

$$P = I_1 + I_2 + 2(I_1 I_2)^{1/2}\cos(\Delta\Phi + \delta_{12}), \tag{3}$$

where I_1 and I_2 are the dissociation signals resulting from one- and two-photon transitions, respectively, and δ_{12} is a molecular phase [17]. The phase difference between the two waves is given by $\Delta\Phi = \varphi_2 - 2\varphi_1$. The solid line in Fig. 7a shows the form $A + B\cos(\Delta\Phi + \Phi_0)$ as a function of $\Delta\Phi$, where A, B, and Φ_0 are adjustable parameters. A $\Delta\Phi$ was determined from the incident angle and refractive index of the quartz plate at 560 nm ($n = 1.459$). The observed oscillation period is in good agreement with the calculated one. This result confirms that the oscillation is solely due to the

interference between the one-photon transition induced by the fundamental light and the two-photon transition induced by the second-harmonic light.

Fig. 7b shows the ratio of the forward and backward ion yields, $R = I_f/I_b$, which was used to estimate whether the angular distribution of the photofragment changed as a function of the relative phase of the two beams [32]. The resulting R showed no phase-dependent behavior within the experimental error. If the photofragments resulting from one-photon and two-photon dissociations have different angular momenta, the interference between the two optical transitions should be observed in the angular distribution of the dissociated products. This interference cannot influence the total dissociation yield, which is the sum of the one-photon and two-photon dissociation yields [18]. Therefore, we conclude that the final state of the two-photon transition induced by the fundamental light is the same as that of the one-photon transition induced by the second-harmonic light and two transitions induce the interference effect in the total dissociation yield.

We now discuss the two-photon transition from the ground state to the $^3\Pi_{0+}(2341)$ state observed in the photodissociation of IBr. When IBr is irradiated with the fundamental light at 560 nm, it is excited to the $^3\Pi_1(2341)$ and $^3\Pi_{0+}(2341)$ states correlated with the I + Br channel. The excited molecules then absorb another photon from the fundamental light and are excited to the $^3\Pi_{0+}(2341)$ state. This two-photon transition from the ground state to the $^3\Pi_{0+}(2341)$ state is dipole forbidden under the selection rule, so that some parity-violating effect must occur. Manakov et al. [19] have proposed the use of a static electric field to achieve the phase control of total ionization yields resulting from interference between a two-photon transition induced by the fundamental light and a one-photon transition induced by the second-harmonic light. The Stark effect induces a mixing of intermediate states with opposite symmetries, leading to the dipole-forbidden two-photon transition. According to this theory, the laser-induced Stark effect is the most likely candidate for the parity-violating effect. Such an effect induced by a strong laser field has been reported in the above-mentioned threshold ionization of atoms [32]. Moreover, it has been reported that strong nanosecond fields (10^{10} to 10^{12} W cm^{-2}) are able to align molecules [33]. When the molecules are aligned with the electric field, the new eigenstates, called pendular states, are formed [34]. These pendular states can be described by the superposition of free rotational states as a result of Stark mixing caused by the electric field. The alignment effect increases the β parameter in the TOF spectrum obtained by one-dimensional photofragment translational spectroscopy. The increase in the β parameter induced by the alignment effect should be observed as an increase in the I* signal. Because this component does not contribute interference, it leads to the decrease of the contrast. In our results, the contrast of oscillation is 0.02 at 1.3×10^{10} W cm^{-2}. By using $I_{max} = I_1 + I_2 + (I_1 I_2)^{1/2}$ and $I_{min} = I_1 + I_2 - (I_1 I_2)^{1/2}$, we can rewrite the contrast of oscillation, C, as $C = 2(I_1/I_2)^{1/2}/(1 + I_1/I_2)$. The expected contrast can be estimated from the ratio between the one-photon signal and the two-photon signal, I_1/I_2. The observed contrast (0.02) is much smaller than the expected contrast (0.52) estimated from the ratio I_1/I_2 (0.08). This discrepancy can be explained by the alignment effect. Considering this situation, it is possible to mix the states of opposite symmetry. Therefore, we conclude that the strong laser field induces a mixing of opposite symmetry in the intermediate $^3\Pi_1(2431)$ or $^3\Pi_{0+}(2431)$ states, leading to the dipole-forbidden two-photon transition that is identical to the one-photon transition induced by the second-harmonic light.

Finally, we discuss the possibility of controlling the branching ratio between the two reaction paths. We have also performed the same experiment in the I + Br channel or the I + Br* channel at 559.46 nm and its second-harmonic light by detecting the ground-state I($^2P_{3/2}$) atoms. We ionized the I($^2P_{3/2}$) atoms by 2 + 1 REMPI using the following electronic transition: I(5p; $^2P^0_{3/2}$) + 2$h\nu$(λ = 279.73 nm) → I(6p; $^2P^0_{1/2}$) [24]. Fig. 8 shows the dissociation yield of I($^2P_{3/2}$) atoms as a function of the quartz plate rotating angle, θ. In this case, the situation is somewhat complicated because all three (2341) states correlate to the I + Br or I + Br* channel. As a result, we detected the mixed signal relevant to two channels. Moreover, when IBr is irradiated with the fundamental light at 560 nm, it is excited to the $^3\Pi_1(2431)$ and $^3\Pi_{0+}(2431)$ states correlated with the I + Br channel, causing the I($^2P_{3/2}$) signal due to the one-photon dissociation. This signal interfered with the detection of the small signal due to the two-photon dissociation. In spite of this situation, the oscillating behavior was observed in the integrated I($^2P_{3/2}$) signal. Although this result is also explained by the same mechanism as the I* + Br channel, we could not determined the branching ratio between relevant channels because the laser wavelengths for the excitation for the I($^2P_{3/2}$) detection and the I*($^2P_{1/2}$) detection are

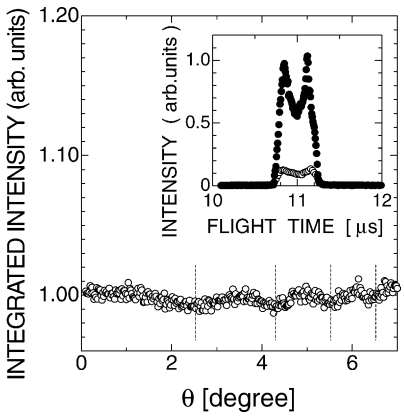

Fig. 8. Dissociation yield of ground-state iodine atoms as a function of the quartz plate rotation angle, θ. The inset shows the TOF spectra of ground-state iodine atoms in the presence of the second-harmonic beam (open circles) and both the fundamental and second-harmonic beams (closed circles).

different, so that we cannot determine the phase lag between the I + Br(Br*) and the I* + Br channel. Further investigations are required to determine whether control of the branching ratio is observed or not.

4. Conclusion

We have shown that the infrared predissociation reaction paths of hydrogen-bonded aniline clusters depend on the excited vibrational mode. This is the second reported example of the mode-selective photoreaction. When a stretching mode of the NH bond that is interacting with another molecule through a hydrogen bond is excited, the fission of this hydrogen bond is enhanced even if that fission is the energetically unfavorable reaction path. This enhancement is due to the strong interaction between the XH stretching vibrational mode and the intermolecular hydrogen bond. Such an infrared predissociation of the hydrogen bond seems to be one way for laser chemists to carry out mode-selective laser chemistry, because hydrogen bonds are widely present in various substances, and to control the hydrogen bond is to control the function of the substance whose secondary structure is determined by hydrogen bond network.

We have investigated the interference effect in the two-color dissociation of IBr using the fundamental and the second-harmonic light. The yield of spin–orbit excited iodine dissociated from IBr molecules shows an oscillating behavior dependent on the relative phase between the fundamental and the second-harmonic light. We conclude that the phase-dependent behavior observed in the total dissociation yield is the source of the interference between the one-photon transition induced by the second-harmonic light and the dipole-forbidden two-photon transition induced by the strong laser fields. Since the absorption coefficient of the two-photon absorption is much larger than that of the three-photon absorption, this scheme of interference seems to be easier to apply than the widely conceived one-photon/three-photon scheme to the control of the photodissociation in the visible to UV absorption region.

References

[1] L.J. Butler, E.J. Hinsta, Y.T. Lee, J. Chem. Phys. 84 (1986) 4104.
[2] L.J. Butler, E.J. Hinsta, S.F. Shane, Y.T. Lee, J. Chem. Phys. 86 (1987) 2051.
[3] M. Shapiro, J.W. Hepburn, P. Brumer, Chem. Phys. Lett. 149 (1988) 451.
[4] G.C. Pimentel, A.L. McClellan (Eds.), The Hydrogen Bond, Freeman, San Francisco, CA, 1960.
[5] T. Nakanaga, F. Ito, Chem. Phys. Lett. 348 (2001) 270.
[6] T. Nakanaga, N.K. Piracha, F. Ito, Chem. Phys. Lett. 346 (2001) 407.
[7] W.S. Warren, H. Rabitz, M. Dahleh, Science 259 (1993) 1581.
[8] H. Rabitz, R. de Vivie-Riedle, M. Motzkus, K. Kompa, Science 288 (2000) 824.
[9] C. Chen, Y. Yin, D.S. Elliott, Phys. Rev. Lett. 64 (1990) 507; C. Chen, D.S. Elliott, Phys. Rev. Lett. 65 (1990) 1737.
[10] S.M. Park, S. Lu, R.J. Gordon, J. Chem. Phys. 94 (1991) 8622.
[11] S. Lu, S.M. Park, Y. Xie, R.J. Gordon, J. Chem. Phys. 96 (1992) 6613.
[12] V.D. Kleiman, L. Zhu, X. Li, R.J. Gordon, J. Chem. Phys. 102 (1995) 5863; V.D. Kleiman, L. Zhu, J. Allen, R.J. Gordon, J. Chem. Phys. 103 (1995) 10800.
[13] G. Xing, X. Wang, X. Huang, R. Bersohn, B. Katz, J. Chem. Phys. 104 (1996) 826.
[14] X. Wang, R. Bersohn, K. Takahashi, M. Kawasaki, H.L. Kim, J. Chem. Phys. 105 (1996) 2992.
[15] L. Zhu, V. Kleiman, X. Li, S.P. Lu, K. Trentelman, R.J. Gordon, Science 270 (1995) 77.
[16] L. Zhu, K. Suto, J.A. Fiss, R. Wada, T. Seideman, R.J. Gordon, Phys. Rev. Lett. 79 (1997) 4108.
[17] J.A. Fiss, L. Zhu, R.J. Gordon, T. Seideman, Phys. Rev. Lett. 82 (1999) 65.
[18] H.L. Kim, R. Bersohn, J. Chem. Phys. 107 (1997) 4546.
[19] N.L. Manakov, V.D. Ovsiannikov, A.F. Starace, Phys. Rev. Lett. 82 (1999) 4791.
[20] H. Ohmura, T. Nakanaga, H. Arakawa, M. Tachiya, Chem. Phys. Lett. 363 (2002) 559.
[21] T. Nakanaga, F. Ito, J. Miyawaki, K. Sugawara, H. Takeo, Chem. Phys. Lett. 261 (1996) 414.
[22] M.J. Frisch, G.W. Trucks, H.B. Schlegel, G.E. Scuseria, M.A. Robb, J.R. Cheeseman, V.G. Zakrzewski, J.A. Montgomery Jr., R.E. Stratmann, J.C. Burant, S. Dapprich, J.M. Millam, A.D. Daniels, K.N. Kudin, M.C. Strain, O. Farkas, J. Tomasi, V. Barone, M. Cossi, R. Cammi, B. Mennucci, C. Pomelli, C. Adamo, S. Clifford, J. Ochterski, G.A. Petersson, P.Y. Ayala, Q. Cui, K. Morokuma, D.K. Malick, A.D. Rabuck, K. Raghavachari, J.B. Foresman, J. Cioslowski, J.V. Ortiz, A.G. Baboul, B.B. Stefanov, G. Liu, A. Liashenko, P. Piskorz, I. Komaromi, R. Gomperts, R.L. Martin, D.J. Fox, T. Keith, M.A. Al-Laham, C.Y. Peng, A. Nanayakkara, C. Gonzalez, M. Challacombe, P.M.W. Gill, B. Johnson, W. Chen, M.W. Wong, J.L. Andres, C. Gonzalez, M. Head-Gordon, E.S. Replogle, J.A. Pople, Gaussian 98, Revision A.7, Gaussian, Inc., Pittsburgh, PA, 1998.
[23] S.G. Lias, J.F. Liebman, R.D. Levin, J. Phys. Chem. Ref. Data 13 (1984) 695.
[24] R.J. Donovan, R.V. Flood, K.P. Lawley, A.J. Yencha, T. Ridley, Chem. Phys. 164 (1992) 439.
[25] D.J. Seery, D. Britton, J. Phys. Chem. 68 (1964) 2263.
[26] M.S. Child, Mol. Phys. 32 (1976) 495.
[27] E. Wrede, S. Laubach, S. Schulenburg, A. Brown, E.R. Wouters, A.J. Orr-Ewing, M.N.R. Ashfold, J. Chem. Phys. 114 (2001) 2629.
[28] K. Jung, J.A. Griffiths, M.A. El-Sayed, J. Chem. Phys. 103 (1995) 6999.
[29] Y.S. Kim, Y. Jung, K. Jung, J. Chem. Phys. 107 (1997) 3805.
[30] W.S. McGivern, R. Li, P. Zou, T. Nguyen, S.W. North, Chem. Phys. 249 (1999) 237.
[31] R.N. Zare, Mol. Photochem. 4 (1972) 1.
[32] B. Sheehy, B. Walker, L.F. DiMauro, Phys. Rev. Lett. 74 (1995) 4799.
[33] J.J. Larsen, H. Sakai, C.P. Safvan, I. Wendt-Larsen, H. Stapelfeldt, J. Chem. Phys. 111 (1999) 7774.
[34] B. Friendrich, D. Herschbach, Phys. Rev. Lett. 74 (1995) 4623.